*16th World Conference on Earthquake Engineering, 16WCEE 2017*

*Santiago Chile, January 9th to 13th 2017*

*Paper N°2635*

*Registration Code: S-A1463283744*

# Cyclic loading behavior of steel chevron braced frames

T. Okazaki[(1)], H. Asada[(2)], M. Midorikawa, and T. Asari

[(1)] *Professor, Hokkaido University, Japan, tokazaki@eng.hokudai.ac.jp*
[(2)] *Assistant Professor, Kobe University, Japan, tokazaki@eng.hokudai.ac.jp*
[(1)] *Professor Emeritus, Hokkaido University, Japan, tokazaki@eng.hokudai.ac.jp*
[(2)] *Assistant Professor, Hokkaido University, Japan, tokazaki@eng.hokudai.ac.jp*

## Abstract

The paper describes an experimental study on the seismic performance of steel concentrically braced frames (CBFs). In Japan, the most common CBF systems place diagonal braces in a chevron (or inverted-“V”) arrangement. Round hollow steel sections (HSS) are popular due to their artistic appeal. While such systems are widely used in commercial buildings, factories, and parking ramps, limited guidance is available in the current code provisions in Japan. Reconnaissance from past earthquakes suggests that these CBFs in Japan are prone to seismic damage. Consequently, three large-scale specimens were tested at Hokkaido University to examine the seismic behavior of chevron CBFs. The specimens placed a pair of braces in a single-bay, single-story moment-resisting frame. The three specimens were identical in dimensions and material selection using a stocky, round-HSS brace with a diameter to-thickness ratio of 18.2. The specimens differed in the design and fabrication of the bracing connections: Two specimens adopted bolted bracing connections that are widely used in Japan, and one specimen adopted a field-welded bracing connection following US recommendations. The specimens were subjected to a cyclic loading protocol based on story-drift ratio that is similar in severity to protocols specified for steel moment-resisting frames. The tests were terminated when one of the two braces fractured or moment-resisting frame distorted severely involving lateral-torsional deformation of the beam and twisting of the column. The test results suggest that chevron CBFs with stocky round-HSS braces and using moment-resisting beam-to-column connections can safely develop large story drifts exceeding 0.03 radians without damage to the bracing connections. Ultimately, severe local buckling in the plastic hinge region led to brace fracture. The force imbalance between the tension and compression braces led to yielding of the beam. Beam deflection forced the braces to deform more in contraction than in elongation: the change in length divided by length of the brace altered between 0.6% in elongation and 3% in contraction. In Specimens 1 and 3, out-of-plane deformation of the braces was accommodated by bending of the gusset plates, which was controlled by design in Specimen 3 but not explicitly intended in Specimen 1. In Specimen 2, the stiffened bracing connection eventually forced twisting of the beam to accommodate brace deformation. All three bracing connections exhibited excellent performance. Although the bolted bracing connections experienced distortion of the splice plates, no bolt slippage was observed. Although the welded bracing connection violated the design requirement for net section fracture, the particular failure mode was not observed in the tests.

*Keywords: steel building systems; concentrically braced frames; chevron arrangement; bracing connections; brace fracture*

## 1. Introduction

Steel concentrically braced frames (CBFs) are widely used in building structures to achieve the lateral stiffness and strength required by seismic design provisions. In seismic-resistant CBFs, the diagonal braces are often placed in the chevron (inversed "V") arrangement in order to accommodate architectural requirements. However, it is well known from past studies [1, 2] that the seismic behavior of chevron CBFs is significantly affected by force unbalance between the tension brace and buckled compression brace. If the beam intersecting the braces is unable to sustain this vertical force, a plastic hinge will form in the beam before the tension brace can develop its yield strength. Consequently, modern seismic code provisions in the US [3] and Japan [4] among other countries require the beams in chevron CBFs to be designed for the condition where the tension brace is fully yielded and the compression brace has buckled and lost much of its strength. Research also shows that the braces in chevron CBFs develop inelastic deformation primarily in contraction. Interestingly, a large-scale test by Uriz [5] suggests that, even if the beam is adequately sized for the force unbalance, the elastic deflection caused by the force unbalance can be large enough to prevent tensile yielding of the brace. In a dynamic loading test by Okazaki et al. [6], elastic beam deflection prevented the brace to yield in tension, and the braces fracture before the expected yielding of the beam occurred.

This paper describes an experimental research program whose objective was to examine the seismic performance of chevron CBFs designed and detailed according to the current requirements and construction practice in Japan. A companion paper by Asada et al. [7] examines the cyclic loading behavior of braces with different the bracing connection arrangement and details.

## 2. Test Plan

### 2.1 Specimens

Fig. 1 shows the configuration of the single-bay, single-story, CBF specimens. The 3-m bay and 2.3-m story height represented 60% scale of a typical building structure. The braces were placed in a V-shape arrangement instead of the inverted-V shape for convenience in testing. The beams were rigidly connected to the column using a pair of continuity plates (through-diaphragm plates) protruding the column and completing the complete-joint-penetration groove weld between the beam flange and through diaphragm plate without a weld access hole. Currently in Japan, this is the most commonly used moment-resisting connection detail. Round-HSS were used for the diagonal braces. The diameter-to-thickness ($D/t$) ratio of 18.2 was within the limiting value for the most stringent category P-I-1 ($D/t \le 36$) per the AIJ recommendations [3] and for highly ductile members ($0.076E/F_y = 63.6$) per the US seismic provisions [4] for round HSS. The slenderness ratio based on the diagonal node-to-node distance of 2,450 mm was 107. The bolted beam splices and bolted bracing connections, using 16-mm diameter F10T bolts, were designed as slip-critical connections.

Fig. 2 shows the bracing connections of the three specimens. At the intersection of two braces and a beam, the gusset plate was provided with a center stiffener and the beam was provided with three stiffeners, in the center and at each end of the gusset plate. Specimens 1 and 2 adopted two variations of bolted bracing connections that are common in Japan, while Specimen 3 adopted a field-welded bracing connection following recent US recommendations [8]. The length of the round HSS was 1,577 mm in Specimens 1 and 2 (as shown in Fig. 1), and 2,100 mm in Specimen 3.

Specimens 1 and 2 had the round-HSS braces welded to a cruciform extension member whose four plates were bolted to a gusset plate, or a fin plate welded to the gusset plate, in double shear. The expected slip resistance of this bolted connection was 1.7 times the nominal tensile yield strength of the brace. Specimen 1 left the three edges of the gusset plate free, while Specimen 2 had the three edges of the gusset plate stiffened. Specimen 3 was designed according to the balanced design proposed by Roeder et al. [8] that ask for an elliptical clearance of eight times the gusset-plate thickness, which generally leads to thinner and smaller gusset plates compared to the straight clearance requirement. The size and total length of the fillet welds in the brace, between the round HSS and extension member or gusset plate, was the same in all specimens. In order to enable the fillet weld connection, four thin slots were prepared at each end of the round HSS. Specimens 1 and 2 had the small remaining slot beyond the extension member filled by welding. Specimen 3 had a pair of slots 40 to 50 mm in length remaining beyond the gusset plate. The segment with reduced cross-sectional area was not reinforced.

Shop welds were made with 1.2-mm diameter Japan Industry Standard (JIS) YGW18 electrodes using the metal active gas welding process, while field welds between the round HSS and gusset plate in Specimen 3 were made with 1.2-mm diameter T49J0T1-1CA-U electrodes (equivalent to AWS E71T-1C) using the gas-shielded flux-cored arc welding process.

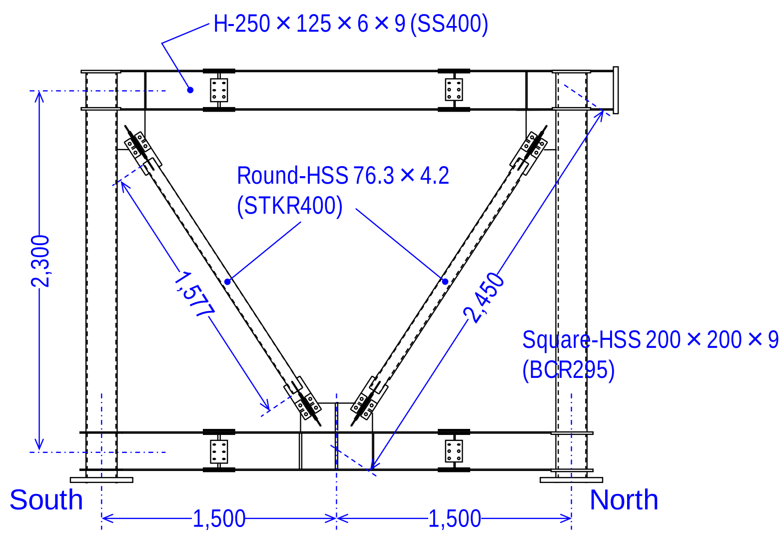


Fig. 1 – CBF specimen (Unit: mm)

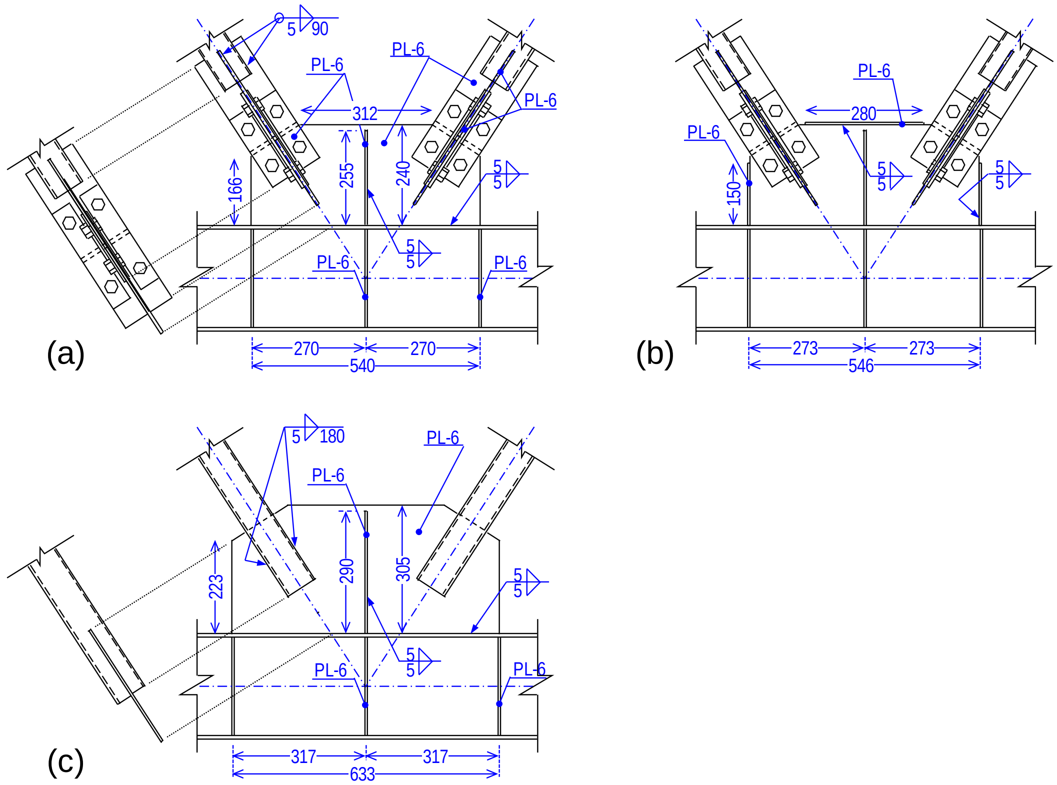


Fig. 2 – Bracing connection between two braces and beam: (a) Specimen 1; (b) Specimen 2; and (c) Specimen 3

Table 1 – Mechanical properties

| Member | Material | Grade | $F_y$ (MPa) | $F_u$ (MPa) | Elongation (%) |
|---|---|---|---|---|---|
| Braces | Round HSS-76.3×4.2 | STKR400 | 374 (343#) | 447 (419#) | 39 |
| Beams | H-250×125×6×9 | SS400 | 343 | 435 | 27 |
| Columns | Square HSS-200×200×9 | BCR295 | 379 | 461 | 39 |
| Plates and stiffeners | PL-6 | SS400 | [1, 2] 351<br>[3] 284 | [1, 2] 450<br>[3] 431 | [1, 2] 32<br>[3] 29 |

Note: The properties for the round HSS-76.3×4.2 and PL-6 are based on tention coupon tests. The properties with superscript (#) for round HSS-76.3×4.2 are based on stub column tests.The properties for the H-250×125×6×9 and square HSS-200×200×9 are taken from mill test reports. Separate properties are listed for PL-6 for Specimens 1 and 2 and for Specimen 3.

### 2.2 Test Setup and Instrumentation

Fig. 3 shows the test setup with a specimen in place. The specimen was supported by two pins, loaded on one side of the upper beam, and braced out of plane at the top and bottom of each column, and in the middle of the beam. Loading was applied by gradually increasing the cyclic story-drift angle from 0.002, 0.00375, 0.005, 0.0075, 0.01, 0.015, 0.02, 0.03, to 0.04 rad. Three cycles were repeated for each story-drift angle up to ±0.01 rad. and afterwards two cycles were repeated for the later cycles.

The applied load and support reactions were measured by load cells. Displacement transducers were used to measure key deformation response such as story drift, brace elongation, out-of-plane rotation and deflection of the brace, and deflection of the lower beam. Strain gauges were placed at selected sections, as shown in Fig. 4, to evaluate the internal force distribution.

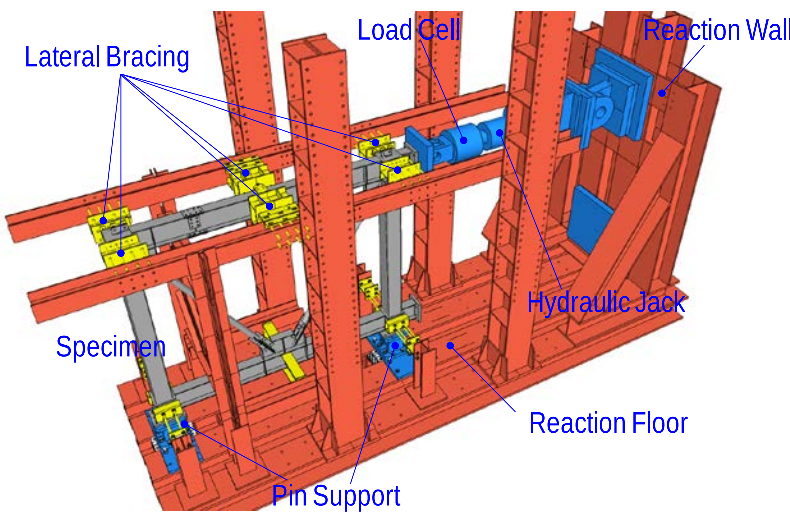


Fig. 3 – Test Setup

## 3. Test Results

Fig. 4 shows the relationship between story shear and story-drift angle measured from each specimen. The reference lines indicate the elastic stiffness computed from basic beam theory, the strength, $H_1$, at brace buckling based on the computed elastic stiffness and brace buckling load stipulated in the current Japanese design recommendations, and the plastic strength, $H_2$, assuming that the tension brace carries the tensile yield strength and the compression brace carries the stipulated reduced strength. The strength estimations were based on the yield strength values listed in table 1. The buckling load and reduced compressive strength were computed based on the node-to-node diagonal distance 2,450 mm and assuming that the braces are pinned at the ends.

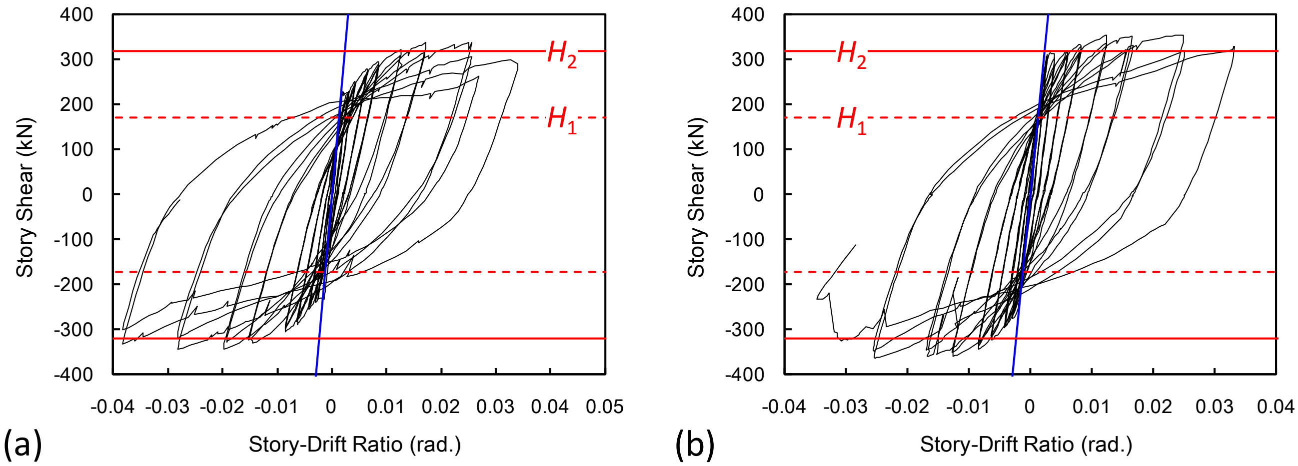


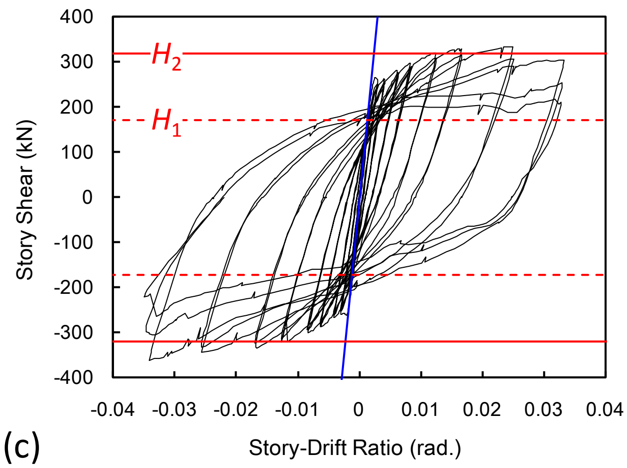


Fig. 4 – Hysteretic response: (a) Specimen 1; (b) Specimen 2; and (c) Specimen 3

Specimen 1 exhibited brace buckling during the first positive excursion of the ±0.00375-rad. cycle. Distortion of the upper and lower beams was observed during the ±0.02-rad. cycles. As the loading amplitude increased, the two braces continued to deform in the same out-of-plane direction. Elliptical folding of the gusset plates, which was not explicitly intended in design, accommodated out-of-plane rotation of the brace. Cupping deformation was observed in the plastic hinge region of the brace during the first positive excursion of the ±0.03-rad. cycle. Subsequently, after three and one half cycles, loading was terminated at the completion of the second ±0.04-rad. cycle when distortion of the beam caused the large twisting of the columns. At this stage, the tensioned braced had developed large cracks but had not fractured.

Specimen 2 exhibited brace buckling during the first positive excursion of the ±0.00375-rad. cycle and severe lateral-torsional deformation of the lower beam during the ±0.02-rad. cycles. Unlike the gusset plates in Specimen 1 that accommodated out-of-plane deformation of the braces, the gusset plates in Specimen 2 developed limited deformation. Meanwhile, the lateral bracing system could not restrain the lower beam from twisting at the brace-to-beam connection. The restraint at the upper bracing connection and twisting of the lower beam seemed to force the plastic hinge to form at a lower position than the middle. Cupping deformation in the plastic hinge region of the brace was observed during the first positive excursion of the ±0.02-rad. cycle. Ultimately, the tensioned brace fractured during the first negative excursion of the ±0.04-rad. cycle.

Similar to the first two specimens, Specimen 3 exhibited brace buckling during the first positive excursion of the ±0.00375-rad. cycle and severe lateral-torsional deformation of the lower beam during the ±0.02-rad. cycles. As intended by design, the gusset plates bent about an elliptical fold line to accommodate out-of-plane deformation of the braces. The fold line straightened in tension during the earlier cycles, but did not entirely straighten during the later cycles. Cupping deformation in the brace was clearly noted during the first positive

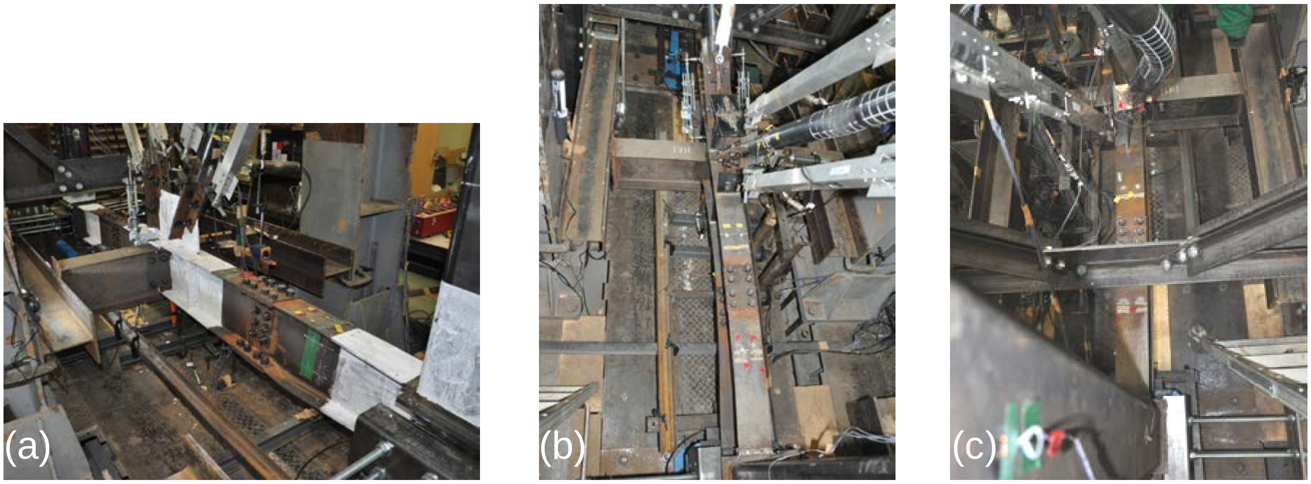


Fig. 5 – Beam deformation: (a) Specimen 1; (b) Specimen 2; and (c) Specimen 3

excursion of the ±0.03-rad. cycle. The brace fractured during the third negative excursion of the ±0.04-rad. cycle.

All three specimens exhibited excellent cyclic-loading behavior. The very large initial stiffness was due to the elastic response of the braces. After the braces buckled, the stiffness gradually approached that of a pure moment frame. In all three specimens, the strength at first buckling of the brace was larger than $H_1$, indicating that the effective length of the brace was shorter than node-to-node distance of 2.450 mm.

Fig. 5 shows the deformation of the lower beam and braces at the first positive excursion of ±0.03-rad. cycles when distortion of the frame was clearly visible in all specimens. The braces interacted with the frame through force imbalance between the tension and compression braces, out-of-plane deformation, and secondary in-plane bending developed in the braces. Strain gauges and deflection measurement indicated that the lower beam yielded near the middle and near the two ends. As the plastic deformation increased, inelastic local buckling of the flanges and web triggered lateral-torsional deformation of the beam. Deformation of the lower beam was most substantial in Specimen 2.

## 4. Observations

Fig. 6 decomposes the relationship between story shear and story-drift angle to the contribution of the moment-resisting frame and that of the two braces. The story shear carried by the moment-resisting frame was determined based on measurements from strain gauges placed on the columns. The story shear carried by the braces was computed by subtracting from the load cell measurement the story shear carried by the columns. In the figure, load $H_b$ indicates the lateral resistance of the braces when the compression brace buckles for the first time, and $H_f$ is the plastic strength of the moment resisting frame disregarding the for unbalance in the middle of the lower beam. As before the buckling strength of the brace was evaluated by taking the node-to-node distance of 2,450 mm as the effective length.

In all specimens, the braces were stronger than $H_b$, which implies that the effective length is substantially shorter than the node-to-node distance. The maximum load carried by the braces was similar between Specimens 1 and 3, but notably larger in Specimen 2. The brace strength at peak drift amplitude was constant in Speicimen 1 but degraded with amplitude in Specimens 2 and 3. The plastic strength of the underlying moment-resisting frame, developed at a story-drift ratio of 0.01 rad., was smaller than $H_f$ in Specimen 1 and barely reached $H_f$ in Specimens 2 and 3.

Fig. 7 compares the deformation of the bracing connection at the first positive excursion of the ±0.04-rad. cycle. The photos view from above the bracing connection in the middle of the lower beam, with the lower beam stretching horizontally and a lateral bracing beam stretching vertically. In all specimens, the braces buckled and deformed primarily in the out-of-plane direction. In Specimen 1, deformation of the gusset plate, although

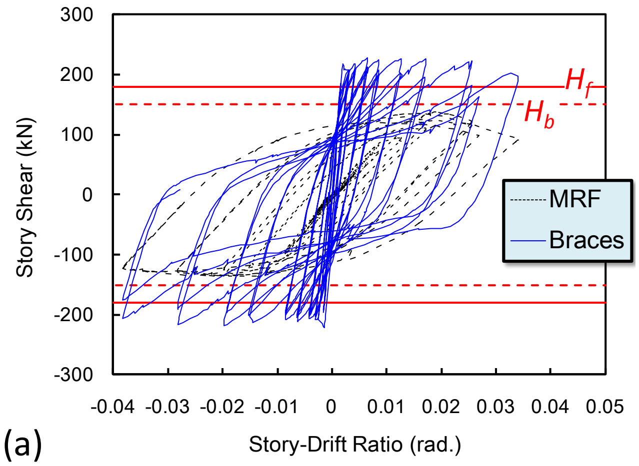


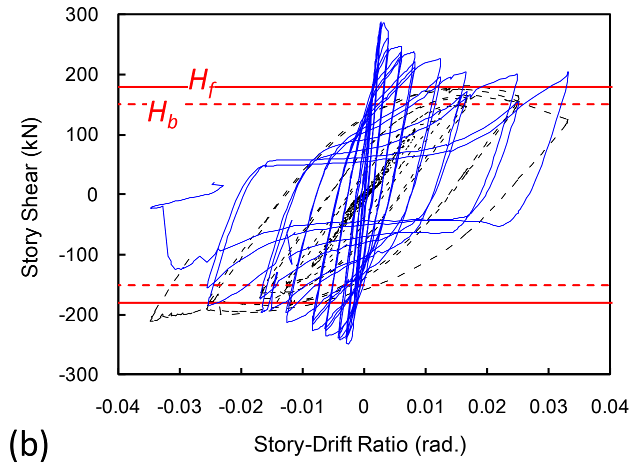


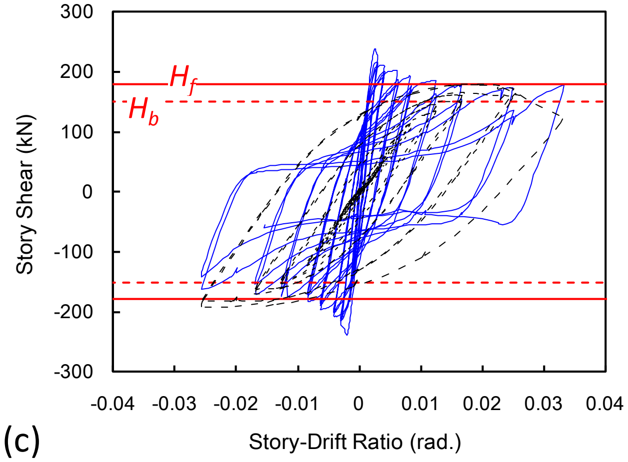


Fig. 6 – Hysteretic response: (a) Specimen 1; (b) Specimen 2; and (c) Specimen 3


Fig. 7 – Bracing connection viewed from above: (a) Specimen 1; (b) Specimen 2; and (c) Specimen 3

unintended, accommodated out-of-plane deformation of the braces. Both braces buckled in the same direction (upwards as seen in Fig. 7a). The two sides of the gusset plate separated by the center stiffener deformed independently. In Specimen 2, the stiffened gusset plate developed limited deformation. Brace deformation was accommodated by twisting and out-of-plane bending of the lower beam as seen in Fig. 7b. The deformation accumulated in a fixed direction during every half loading cycle (see Fig. 5b). Rigid body rotation of the combined bracing connections forced the braces to deform in opposing directions. The gusset plates in Specimen 3 was designed to provide minimal restraint to out-of-plane deformation of the braces. This design goal was met adequately as evidenced by Fig. 7c. As in Specimen 1, the braces buckled in the same direction (downwards as seen in Fig. 7c).

Fig. 8 views the bracing connection at the same stage from the side. In Specimens 1 and 3, no discernible damage in the bracing connections was observed at the end of the test. In Specimen 2, at the end of both braces, small cracks were developing at the weld termination of the gusset edge stiffeners and at the end of the find plate, at locations indicated in Fig. 8b with arrows.

Fig. 9 shows key locations of the bracing connections near the end of the test. Regardless of the large bending deformation and gap opening between plates seen in Fig. 9a, the bracing connections of Specimens 1 and 2 did not slip in the bolted connection. Fig. 9b shows an upper bracing connection in Specimen 2 where cracks formed at the weld termination of gusset edge stiffeners and at the end of the fin plate. Net section fracture of the round HSS at end of the slot, which was not filled with welding and was not reinforced by cover plates, was a design concern for Specimen 2. Despite the concern, no cracks formed at this location. However, there is no assurance that these welded connection will perform well in brace arrangements other than the chevron where the braces will fully develop in tension.

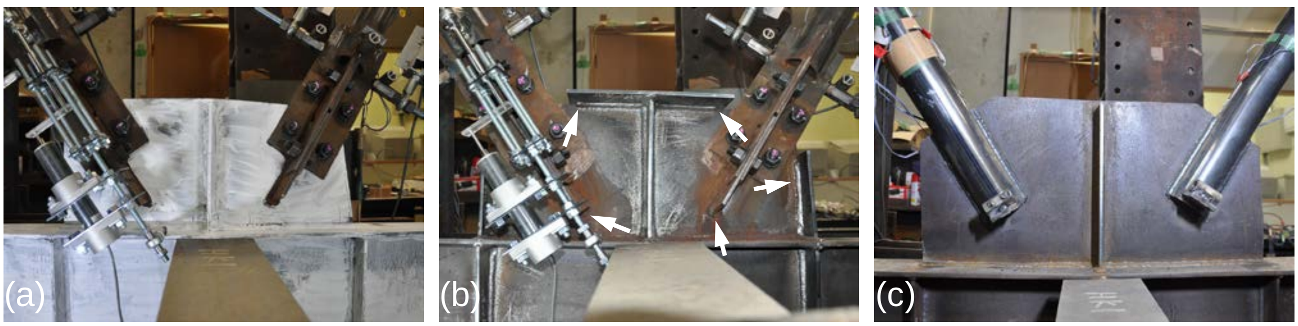


Fig. 8 – Bracing connection viewed from side: (a) Specimen 1; (b) Specimen 2; and (c) Specimen 3


Fig. 9 – Close-up view of bracing connections: (a) Specimen 1; (b) Specimen 2; and (c) Specimen 3

## 5. Summary

Specimens comprising a single-story, single-bay moment resisting frames with round-HSS braces placed in a chevron arrangement was subjected to cyclic loading. The three specimens were identical expect for the bracing connection details. Two specimens adopted bolted connections that are commonly used in Japan, while the third specimen adopted a field-weld connection following US recommendations. Key results and observations are summarized below:

- All three specimens developed an inelastic story drift exceeding 0.03 rad. before loading was terminated due to fracture of the tension brace or severe distortion of the moment-resisting frame.

- As reported in earlier studies of chevron braced frames, the braces deformed more in contraction than in elongation. The change in length divided by length of the brace altered between 0.6% in elongation and 3% in contraction.
- The relatively small diameter-to-thickness ratio (*D*/*t*) of 18.2 contributed to the large deformation capacity. The braces generally fractured three full cycles after cupping deformation was first observed in the plastic hinge region.
- The performance of the two bolted connection types suggests that there is limited merit in stiffening the gusset plates. In this program, the unstiffened gusset plate accommodated out-of-plane deformation of the braces by, although unintended in design, forming fold lines in the gusset plates. The stiffened gusset plates forced twisting of the beam to accommodate brace deformation. Fracture of the brace occurred at an earlier stage in the stiffened gusset plate. While the unstiffened gusset plate remained undamaged at the end of the test, the stiffened gusset plate formed cracks at end of the fin plates.
- All three bracing connections exhibited excellent performance. Although the bolted bracing connections experienced distortion of the splice plates, no bolt slippage was observed. Although the welded bracing connection violated the design requirement for net section fracture, the particular failure mode was not observed in the tests. However, there is no assurance that the welded connection will perform well in other brace arrangements where the braces will fully develop in tension.

## 6. Acknowledgements

Funding for the experimental project presented in this paper was provided by the Research and Education Promotion Program of the Japan Iron and Steel Federation. Yuto Kameoka and Keisuke Inoue contributed to the planning and execution of the tests. The opinions expressed in this paper are those of the authors and do not necessarily reflect the views of the individuals and organizations mentioned herein.

## 7. References

[1] Wakabayashi M, Shibata M, Imamura T, Nishino T (1981): Experimental study o the hysteretic behavior of K-type braced frame. *Bulletin of the Disaster Prevention Research Institute*, **24** (B-1), 171-183.

[2] Muto K, Endo K, Goto Y (1981): A demonstrative study of aseismic design on a large turbine building with K-type braced frame – Part 1 Experimental study of elasto-plastic characteristic of K-type braced fame. *Journal of Structural and Construction Engineering*, Architectural Institute of Japan, 356, 171-183.

[3] Architectural Institute of Japan (AIJ) (2010): *Recommendations for Limit State Design of Steel Structures*. AIJ, Tokyo, Japan (in Japanese).

[4] American Institute of Steel Construction, Inc. (AISC) (2010): *Seismic Provisions for Structural Steel Buildings*. ANSI/AISC Standard 341-10. AISC, Chicago, Illinois, USA.

[5] Uriz P (2005): Towards earthquake resistant design of concentrically braced steel structures. *Ph.D. Dissertation*, Dept. of Civil and Environmental Engineering, Univ. of California, Berkeley, CA, USA.

[6] Okazaki T, Lignos DG, Hikino T, Kajiwara K (2013). Dynamic response of a chevron concentrically braced frame, *Journal of Structural Engineering*, American Society of Civil engineers, **139** (4), 515-525.

[7] Asada H, Okazaki T, Tanaka T, Hashioka A (2017): Effect of bracing connection on the cyclic loading behavior of round-HSS braces, 16th World Conference on Earthquake Engineering, Santiago, Chile.

[8] Roeder CW, Lumpkin EJ, Lehman DE (2011): A balanced design procedure for special concentrically braced frame connections. *Journal of Constructional Steel Research*, ***67***, 1760-1772.